SSRG International Journal of Electronics and Communication Engineering
ISSN: 2348-8549/ https://doi.org/10.14445/23488549/IJECE-V11I7P113

Volume 11 Issue 7, 128-140, July 2024

Original Article

Band Pass Filter Based on Double Split Ring Resonator for 5G Applications

Asari Gauravkumar Ravindra[1], Shah Milind Siddharthbhai[2]

[1]*Gujarat Technological University, Gujarat, India.*
[2]*Department of Electronics and Communication Engineering, Shantilal Shah Engineering College, Gujarat, India.*

[1]*Corresponding Author : gauravasari24@gmail.com*

Received: 09 May 2024 Revised: 09 June 2024 Accepted: 08 July 2024 Published: 27 July 2024

Abstract *- Compact, affordable, high-performing, and easily integrable microwave filters are essential for advancements in communication. This study investigates a planar band pass filter that is loaded with a double split ring resonator that serves as a metamaterial for 5G applications. The initial phase of the work focuses on verifying the metamaterial unit cell using the Nicholson-Ross Weir technique, which provides evidence of the split ring resonator's negative permittivity and negative permeability. The band pass filter in the second section is designed using ANSYS HFSS software on a FR4 substrate. The substrate has a dielectric constant of 4.4, a loss tangent of 0.025, and a thickness of 1. 6mm. Parametric analysis is conducted to optimize the dimensions of the split ring resonator and the band pass filter. The band pass filter, which utilizes metamaterial, exhibits a return loss of 30.41dB and an insertion loss of 1.77dB at a frequency of 4.71 GHz. Similarly, at a frequency of 6 GHz, it demonstrates a return loss of 27.91 dB and an insertion loss of 1.28 dB. These characteristics make it appropriate for sub-7GHz 5G NR-Light applications. The band pass filter is compact, measuring 21.2mm in length and 11.8mm in width.*

Keywords *- Double Split Ring Resonator, Band pass filter, Permittivity and permeability, S parameters, ANSYS HFSS.*

1. Introduction

Researchers have shown interest in creating a miniature, cost-effective, high-performance band pass filter that can be easily integrated with other circuit elements in light of the advancements in 5G technology. With the increasing number of communication devices, there is a need for greater bandwidth, faster data transfer rates, and reduced latency [1]. The high 5G band is ideal for transmitting large amounts of data at a fast rate. However, it has a limited range compared to the mid and low 5G bands [2]. Conversely, the lower frequency range of 5G offers extensive coverage but exhibits slower data transmission speeds and higher latency. The mid-range 5G frequency is regarded as optimal due to its ability to transmit massive amounts of data over long distances [3]. Unlike existing 5G-based services, 5G NR-Light provides reduced complexity, enabling the creation of devices that consume less power, are more cost-effective, and have smaller physical dimensions.

Filter-based communication systems have been extensively employed in industrial and commercial applications. However, it is crucial to minimize the intricacies and expenses associated with the design and production of systems that utilize filters [4-6]. In recent years, cellular systems have undergone evolutionary upgrades in the form of smart homes, telemedicine, IoT, and smart cities. These advancements require a filter to ensure that there are no space limitations, as vendors demand slim and portable devices [7].

A microstrip-SIW-SIPW-SIW-microstrip band pass filter is designed in [4]. Etching double arrays of rectangular slots on both metal layers of SIW forms the Substrate Integrated Plasmonic Waveguide (SIPW). The electrical properties of the designed filter are distorted by mode conversion and impedance mismatch between the structures. In [5], etching hourglass- and fishbone-shaped transition grooves on the top metal simplifies mode conversion. Linear tapered fishbone groove structure is developed to reduce the impedance mismatch between the microstrip line and hourglass-shaped groove structure SSPP part. In [6], the plasmonic metamaterial is used to create SSPP band pass filters with four sections: CPW input, mode converter, Tx line section, and resonator structure.

Obtaining an equivalent circuit becomes difficult for the complex filter architectures [4-6] grounded via holes. In addition, mode conversion and impedance matching reduce return loss to 10-15dB, while insertion loss increases more than 2 dB. Spurious responses, mainly from the second harmonic, can be reduced using coupled sections. Since they are made of quarter or half-wavelength resonators, they are large. Filters [4-6] are 67.1mm x 18.0mm, 34.3mm x 12.2mm, and 260.0mm x 40.0mm in size, respectively.

The band pass filter presented in [8] utilizes a split ring resonator with circular geometry. To enhance the efficiency of the filter described in [8, 9] suggested a series-connected band-pass filter consisting of split ring resonators with square-shaped geometry. The filter enhanced the return loss and insertion loss by 58% and 84%, respectively. As a companion approach, [10] suggested connecting square split ring resonators in parallel, which leads to a reduced filter size compared to [9]. Recent research [11-14] indicates that split ring resonators play a crucial role in the development of band-pass filters for 5G applications. An advantage of using a split ring resonator is that its size is smaller than the free space wavelength at resonance [15].

This paper presents the design of a novel band pass filter that utilizes a split ring resonator acting as a metamaterial structure, which is notable for its compact size and enhanced electrical characteristics compared to filters in [4-6]. The study commences with an introductory section, followed by a literature review. It then proceeds to describe the metamaterial resonator and illustrate its metamaterial characteristics using the Nicholson Ross Weir (NRW) technique [16]. The subsequent section pertains to the design of the proposed band pass filter. Finally, the results are examined.

2. Literature Review

Defitri & Munir [8] employed a Roger RT/Duroid 5880 dielectric substrate with a height of 0.50mm to create a band pass filter for the X band. The filter incorporated a circular split ring resonator. The simulation findings indicate that the band pass filter exhibits an insertion loss of 2.76 dB and a return loss of 15.23 dB at a centre frequency of 9.02 GHz. The parametric analysis, conducted using ANSYS HFSS software, found that narrower rings exhibit lower centre frequencies. The centre frequency increases as the distance between the ends of the ring and the gap between the rings increases.

Zhao et al. [10] created a band pass filter by placing two square-shaped split ring resonators on the upper and lower sections of a microstrip line. The filter utilizes a tunable device. The filter's operating frequency decreases as the capacitance of the varactor diode increases. When the capacitance increases from 0.1 pF to 1.0 pF, the centre frequency reduces from 11.8 GHz to 10.8 GHz. The maximum value of the transmission coefficient is 0.37 dB, whereas the minimum value of the reflection coefficient is 35 dB.

Syahral & Munir [11] developed a band pass filter by designing three square-shaped split ring resonators, each consisting of two rings, for the 2.4 GHz frequency. These resonators were fabricated on a 1.9 mm thick Rogers RT/Duroid 6010/6010LM substrate. The insertion loss is 3.84 dB, and the return loss is 26.07 dB. The study demonstrates the impact of modifying different ring characteristics, such as ring length, ring width, and ring gap, on frequency shift, return loss, and insertion loss. When the length and width increase by 0.2 mm, the return loss shows random variations, but the insertion loss remains constant at approximately 1.7 dB. As the gap widens by 0.2 mm, the insertion and return losses exhibit random variations. In the first two situations, the centre frequency shifts by 100 MHz, whereas in the third case, it shifts up to 200 MHz.

Umeshkumar and Kumar [17] have created an ultra-wideband band pass filter by utilizing three distinct structures: a square patch resonator, a split ring resonator, and a dual shunt ring resonator placed between two parallel coupled lines. The filter utilizes RT/Duroid 6002 as its substrate, with a thickness of 0.12 mm and a dielectric constant of 2.94. The filter is specifically designed to operate within the frequency range of 22 GHz to 29 GHz, with a central frequency of 25.5 GHz. The filter simulation is performed using ANSYS HFSS software. The filter that has been developed is specifically designed for utilization in automotive RADAR applications. The first design of the filter incorporates two coupled microstrip lines and two identical shunt ring resonators. The return loss is 14 dB, and the insertion loss is 0.4 dB. The second filter consists of two coupled microstrip lines and a dual split ring resonator. The return and insertion losses are 16 db and 0.39 dB, respectively. The third filter is constructed using two square patch resonators that are connected to two coupled microstrip lines. The return loss is 36 dB, and the insertion loss is 0.3 dB.

Salim et al. [18] designed a band pass filter by utilizing open loop resonators on a Rogers RO3010 substrate that is 1.5 mm thick and has a relative permittivity of 10.2. This filter was specifically developed for Bluetooth and WLAN applications. An analysis is conducted using CST Studio software to examine the impact of filter parameters, including the placement of transmission zeros, s parameters, and centre frequency. At a frequency of 2.40 GHz, the measured return loss is 26 dB, and the insertion loss is 0.8 dB. The final transmission zeros are located at frequencies 2.17 GHz and 2.63 GHz, demonstrating a substantial cut before and after the passband.

Abdul Hassain et al. [19] have developed a band pass filter using ANSYS HFSS software. The filter consists of a parallel coupled line loaded with two stepped impedance stubs, CSRR and SRR. Initially, a band pass filter with a parallel coupled line is created at a frequency of 1 GHz, utilizing an FR-4 substrate that has a height of 1. 6 mm. Spurious frequencies appear at double the fundamental frequency. SRR and CSRR are added to the design of the band pass filter to prevent spurious frequencies. However, the inclusion of the SRR and CSRR adversely affects the insertion loss. As a solution, two-stepped impedance stubs are incorporated to improve the performance within the pass band.

Nasiri et al. [20] have designed a highly compact bandpass filter for IMT-E and WiMAX applications using CST Microwave Studio. The filter is based on a square-shaped complementary split ring resonator. The filter is constructed using a substrate made of FR-4 material that has a thickness of 1.6 mm and a dielectric constant of 4.4. Upon initial investigation of the CSRR, a negative permeability is noted within the frequency range of 2.5-4 GHz. The band pass filter provides excellent transmission quality throughout the frequency range of 2.8 GHz to 5.3 GHz, with a wide pass band. Additionally, it has favourable return loss and insertion loss.

Becharef et al. [21] utilized ANSYS HFSS software to construct a compact band pass filter using a circular complementary split ring resonator. The filter is designed on a substrate with a thickness of 0.81 mm and a dielectric constant of 3.1. The filter consists of two metal stubs and one complementary split ring resonator cell. This study looks into how variations in the filter's physical dimensions affect its sensitivity to frequency response. The frequency spectrum exhibits minor shifts as the length of the gap changes. The positioning of the filter's two stubs had a significant effect on frequency responses, resulting in a performance improvement of 15 dB. The difference in the stub widths and line widths results in a minor change in frequency but diminishes the performance of the bandwidth.

Topaloğlu [22] has constructed a model utilizing a split ring resonator consisting of three elements. The ANSYS HFSS software is used to analyse the model over a frequency range of 1 GHz to 20 GHz. The study includes measurements of s parameters and the determination of effective permittivity. An investigation is conducted to analyse the electromagnetic field using Finite Element Analysis (FEA). The investigation focuses on examining the magnetic field strength, electric field, and surface current density. The split ring resonator exhibits metamaterial properties within the frequency range of 10.1 GHz to 15.5 GHz, making it suitable for wireless applications. The magnitude of the s-parameters demonstrates excellent electrical performance across the range. The EM analysis indicates the electric and magnetic field strengths are concentrated on the rings and decrease in the dielectric substrate. Both positive and negative poles are detected due to the relatively uniform surface current density. The resonance frequency will vary based on changes in the capacitance and inductance values of the split ring resonator rings by an uneven distribution of surface current density.

Vineetha et al. [23] developed a triple band band-pass filter for WLAN applications using the ANSYS HFSS software. The filter was created utilizing a split ring resonator. The filter is built on a FR-4 substrate, which has a dielectric constant of 4.3. The split ring resonator consists of three rings, and parametric analysis is employed to adjust the length and width of these rings. The study revealed that when the length and width of all rings increased, there was a decrease in insertion loss and an increase in return loss. The filter exhibits an insertion loss of 0.7 dB, 1.27 dB, and 2.1 dB at frequencies of 2.4 GHz, 4.5 GHz, and 5.2 GHz, respectively. Additionally, it demonstrates a reflection loss of 22.7 dB, 23 dB, and 16.5 dB at the same frequencies.

Sagadevan et al. [24] have created a band pass filter that incorporates a split ring resonator with variable centre frequency and bandwidth. This filter is designed for applications in imaging, wireless communication, and spectroscopy. The COMSOL Multiphysics software is utilized for the simulation. Modifications are made to the ring width, inter-ring spacing, and gap to analyse the frequency response of the split ring resonator with a square configuration. The resonance frequency varies from 3.6 THz and 7.2 THz, while the bandwidth extends from 1.1 THz to 3.4 THz as the ring width changes. The bandwidth can vary between 0.9 THz and 3.3 THz, depending on the spacing between the rings. Similarly, the resonant frequency can range from 3.8 THz to 7.0 THz. By varying the gap, the bandwidth expands from 0.9 THz to 3.3 THz, while the resonant frequency varies between 3.8 THz and 6.8 THz.

Nasiri et al. [25] utilized CST Microwave Studio and ADS Agilent software to create a compact band stop filter with a double split ring resonator specifically designed for GSM applications. The filter is built on a low-cost FR-4 substrate, which has a dielectric constant of 4.4. At the resonant frequency, the designed filter exhibits negative permittivity and permeability. Upon closer inspection, it is evident that the filter has a reject band that extends from 1.5 to 2.3 GHz.

This paper has incorporated two square-shaped double split ring resonators placed anti-parallel between the U-shaped filter to achieve a wide pass band characteristic. Physical parameters of the S-DSRR, like ring length, ring width and gap, are varied to investigate frequency shift, transmission, and reflection coefficients. The parameters are optimized to further improve the return and insertion loss as well as having a sharp cut before and after the pass band.

3. Metamaterial Resonator

The key features of the material, notably its magnetic permeability (μ) and electric permittivity (ε), have a significant influence on the performance of microwave circuits. The materials are categorized according to their inherent characteristics. Materials that are referred to as double-positive have the characteristic of possessing both positive permittivity and permeability. According to Veselago's theory [26], if both quantities have negative values, they are double negative materials or left-handed materials. Pendry's demonstration of a resonant double ring [27], thirty years later, is considered the key element of the first metamaterial ever created. Smith produced his work in 2000 [28].

Figure 1 shows the proposed square split ring resonator, and Table 1 provides a detailed enumeration of its dimensions. The split ring resonator is called a dual split ring resonator because, as Figure 1 illustrates, it consists of two rings. Four distinct features characterize the ring. The first is the length of the inner and outer rings. The second is the width of the inner and outer rings.

The third is the separation between the inner and outer rings, known as interring spacing. Fourth is the distance between the edges of the square open loop, known as the ring gap. The SRR unit can resonate at wavelengths larger than the diameter of the rings due to the splits in the rings. The second split ring, which is within and oriented in the opposite direction from the first, serves to concentrate the electric field and significantly decreases the resonant frequency by creating a significant amount of capacitance in the small region between the rings [29].

Figure 2 illustrates the equivalent circuit for the split ring resonator, which is modelled as an LC circuit [30]. Each ring can be represented as a solenoid, and the inductance of the ring is denoted by L_m. C_m denotes the capacitance resulting from the distance between the rings, whereas C_{gap} represents the capacitance produced by the plane that divides the two rings.

The inductance of the rings is represented by Equation (1) [30].

$$L_m = \frac{\mu_0 Z}{S}(P_1 + U) \tag{1}$$

Where, P_1 and U are the outer and the inner ring lengths, S is the width of the ring, and Z is the gap between the rings.

The capacitance between the rings is represented by Equation (2) [30].

$$C_m = \frac{A\varepsilon_0\varepsilon_r S(2P_1+2U-Y)}{2Z} \tag{2}$$

Where, A is the equilibrium constant, ε is the permittivity, and Y is the gap.

Finally, C_{gap} is represented by Equation (3) indicates [30].

$$C_{gap} = \frac{\varepsilon_0\varepsilon_r t}{Y} \tag{3}$$

Where t is the thickness of the ring.

The resonant frequency based on the geometrical parameters of the square split ring resonator can be expressed as

$$f_r \approx \frac{1}{2\pi(L_m C_m)^{1/2}} \tag{4}$$

The FR4 substrate that the resonator is constructed on has a thickness of 1.6 mm, a dielectric constant of 4.4, and a loss tangent of 0.025.

The Nicolson-Ross-Weir (NRW) approach [16] and ANSYS HFSS software are employed to extract the permittivity and permeability, which are then used to demonstrate the metamaterial properties of the split ring resonator seen in Figure 1. Equations (5) and (6) form the fundamental framework for the approach. Figures 3 and 4 demonstrate the effective permittivity and permeability of the split ring resonator that has been produced. These figures indicate that the resonator functions in a manner that is similar to that of a metamaterial.

$$\mu_r = \frac{2}{jk_0 t}\frac{(1-V_2)}{(1+V_2)} \tag{5}$$

$$\varepsilon_r = \frac{2}{jk_0 t}\frac{(1-V_1)}{(1+V_1)} \tag{6}$$

Where, k_0 is the wavenumber, t is the thickness of the substrate, $V_1 = S_{11} + S_{12}$ *and* $V_2 = S_{12} - S_{11}$

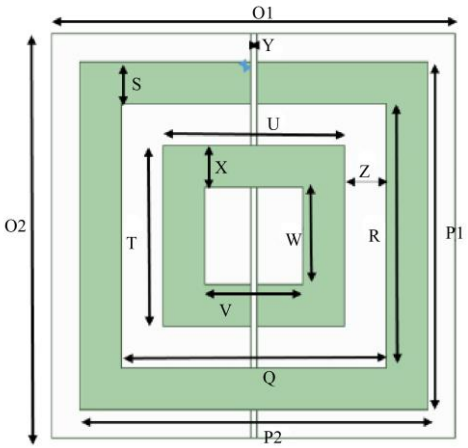

Fig. 1 Split ring resonator

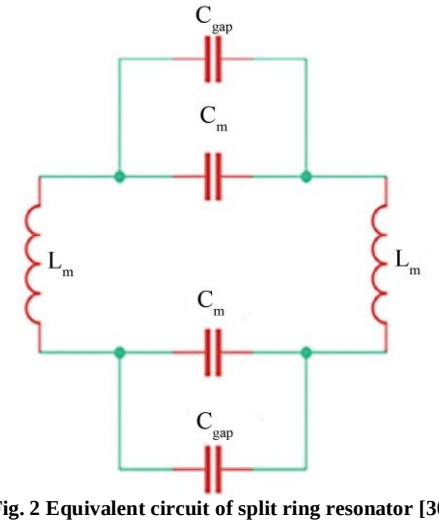

Fig. 2 Equivalent circuit of split ring resonator [30]

Figure 5 displays the insertion and return losses of the split ring resonator. At a frequency of 4.74 GHz, the device exhibits an insertion loss of 0.48 dB and a return loss of 20.36 dB, indicating its functionality as a metamaterial.

The ANSYS HFSS software is utilized to do a parametric study of the split ring resonator, considering different lengths and widths.

The parametric analysis of the split ring resonator for different lengths and widths is depicted in Figures 6 and 7. The center frequency undergoes a shift of 100MHz in response to changes in both the length and width. Conversely, the insertion loss is decreasing while the return loss is increasing.

Table 1. Dimensions of the split ring resonator in mm units

Parameter Symbol	Parameter Name	Value
O_1 and O_2	Substrate Length and Width	5.8
P_1 and P_2	Outer Ring Length and Width	5.0
Q and R	Outer Ring's Inner Length and Width	3.8
S and X	Outer and Inner Ring Width	0.6
T and U	Inner Ring Length and Width	2.6
V and W	Inner Ring's Inner Length and Width	1.4
Y	Outer and Inner Ring Gap	0.1
Z	Gap Between Two Rings	0.6

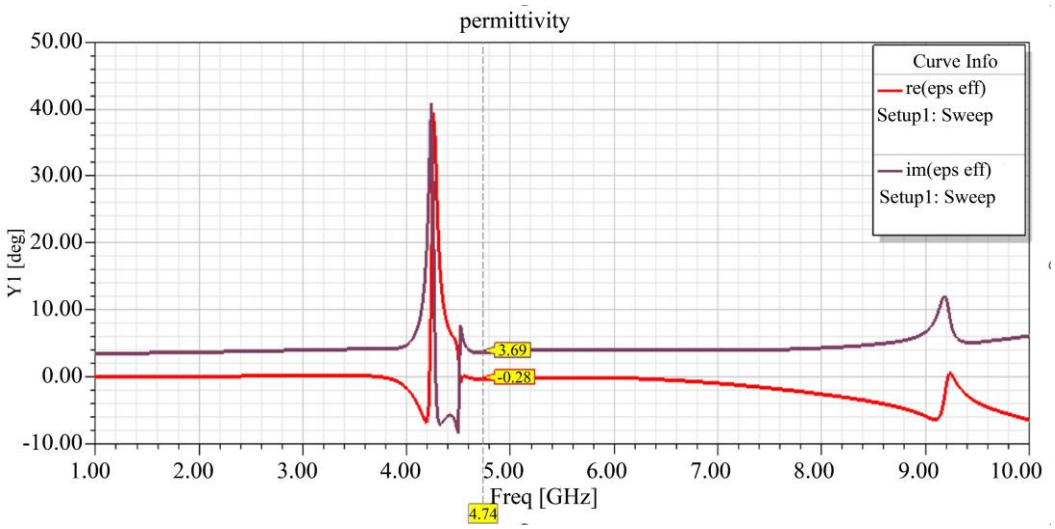

Fig. 3 Effective permittivity of the split ring resonator

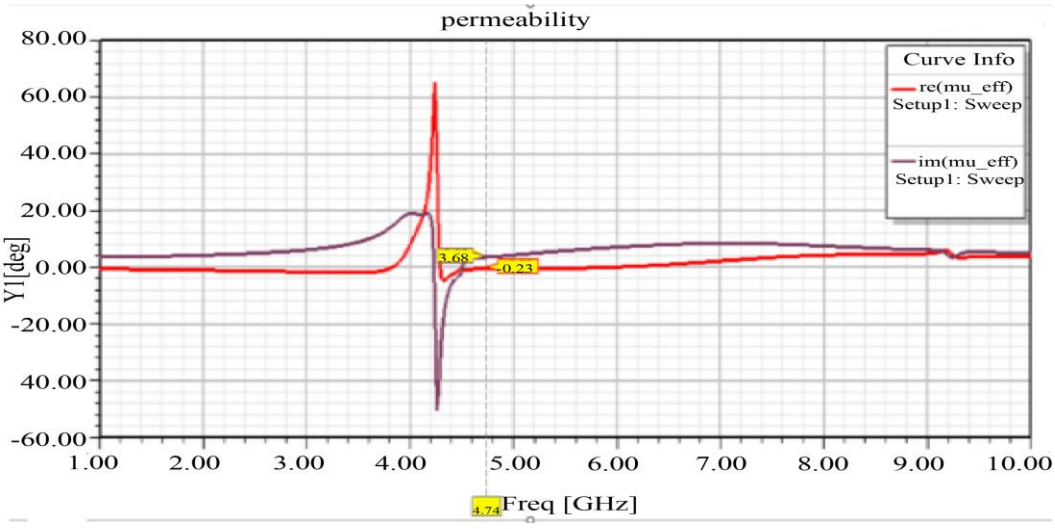

Fig. 4 Effective permeability of split ring resonator

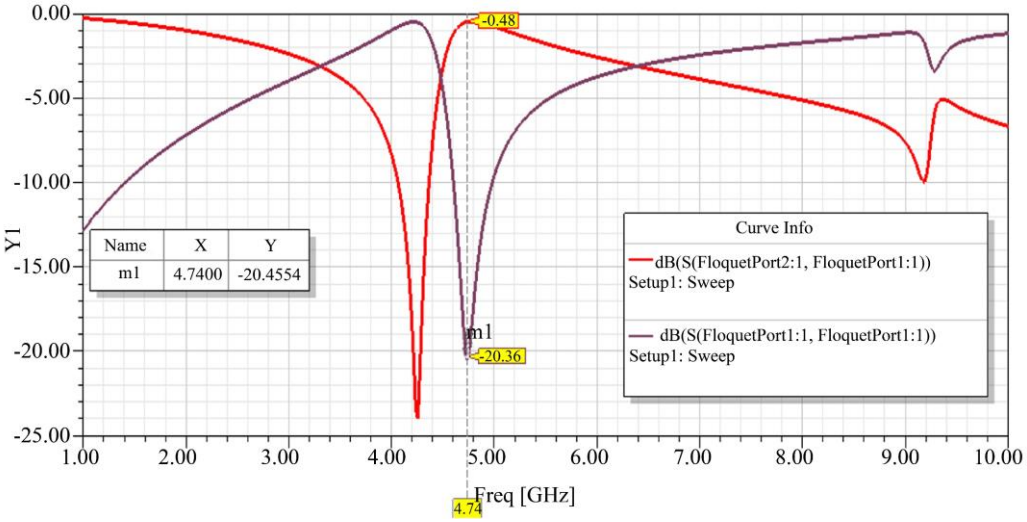

Fig. 5 S_{11} and S_{21} of split ring resonator

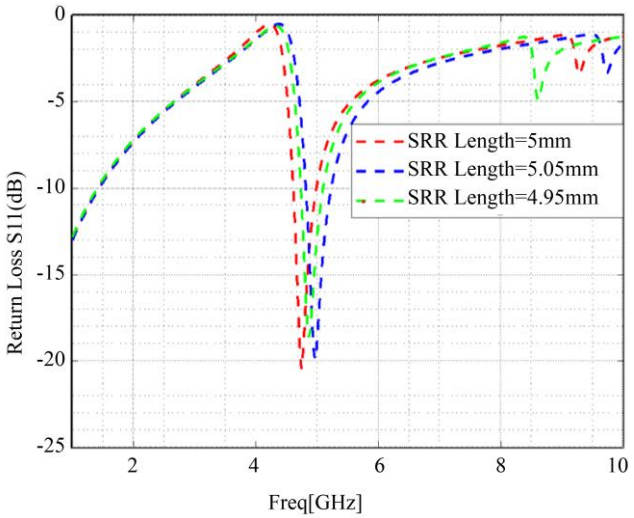

Fig. 6(a) S_{11} of split ring resonator by varying the length

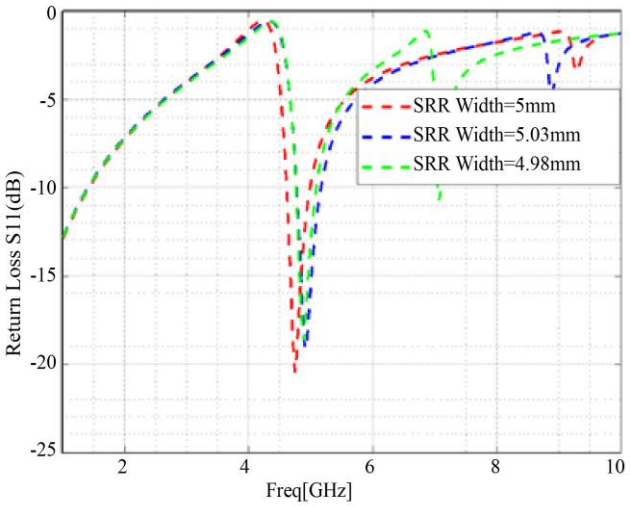

Fig. 7(a) S_{11} of split ring resonator by varying the width

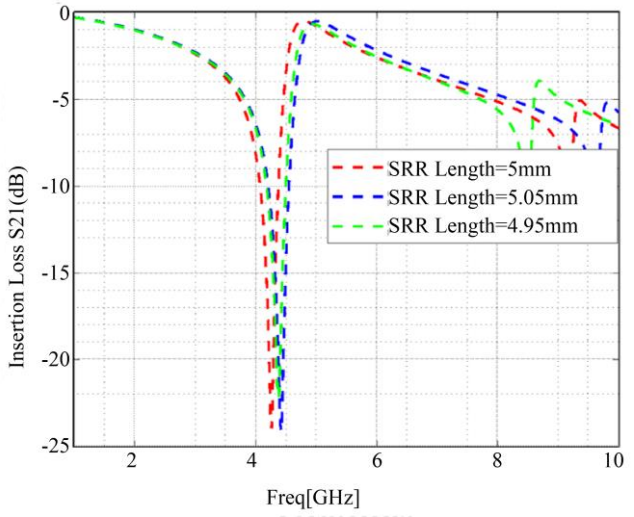

Fig. 6(b) S_{21} of split ring resonator by varying the length

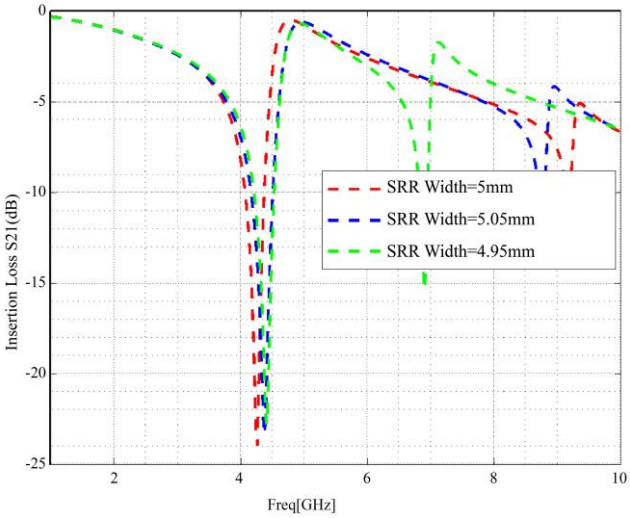

Fig. 7(b) S_{21} of split ring resonator by varying the width

4. Proposed Band Pass Filter Design

The steps for designing a band pass filter are divided into four components. After making an FR4 substrate that is 1.6 mm thick, has a dielectric constant of 4.4, and a loss tangent of 0.025, as shown in stage 1 of Figure 8(a), a cross-shaped slot is made on the ground plane.

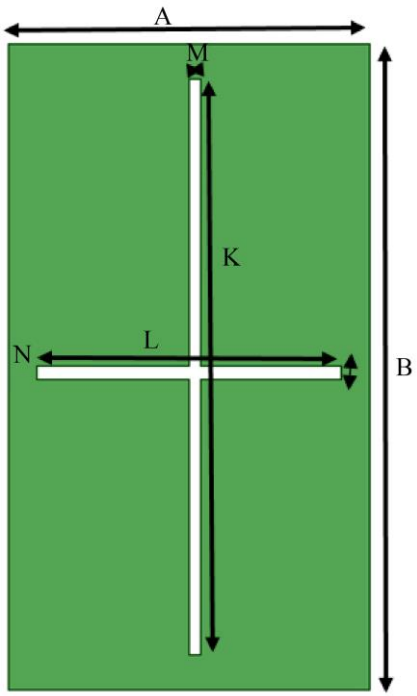

Fig. 8(a) Stage-1 of the band pass filter design

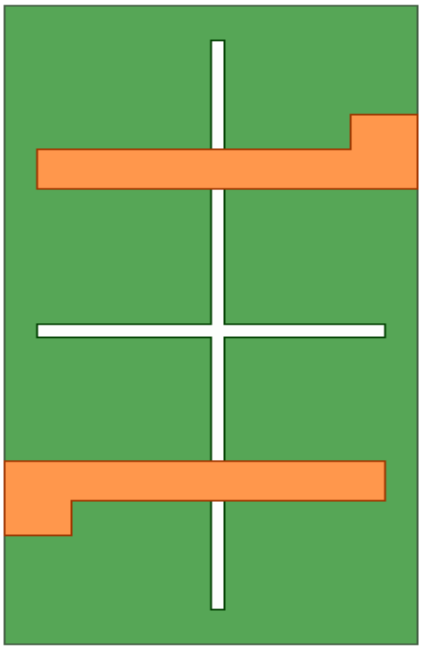

Fig. 8(b) Stage-2 of the band pass filter design

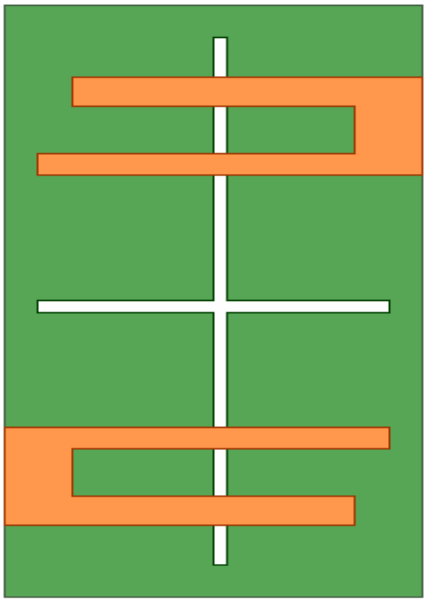

Fig. 8(c) Stage-3 of the band pass filter design

This aperture in the shape of a cross is referred to as the defective ground structure. Any etching that occurs in the ground plane underneath the microstrip line changes the effective capacitance and inductance of the microstrip line by increasing slot resistance, capacitance, and inductance [31].

In the second part, a microstrip feed line in the shape of a "L" is constructed with an impedance of 50 Ω. This is shown as stage 2 in Figure 8(b). The third part develops a U-shaped filter, denoted by stage 3 in Figure 8(c).

The last step is to add two square split ring resonators that work as metamaterial and are spaced 1.2 mm apart, as shown in stage 4 of Figure 8(d). The filter dimensions are shown in Table 2.

The ANSYS HFSS software is used to perform parametric analysis to optimize the length and width of the split ring resonator, which is integrated into the band pass filter, as depicted in Figures 9 and 10. As the dimensions of the ring increase, the return loss improves while the insertion loss remains constant at approximately 0.9 dB.

Table 2. Dimensions of the proposed band pass filter in mm units

Parameter Symbol	Value	Parameter Symbol	Value
A	11.8	H	1.0
B	21.2	I	11.0
C	3.4	J	1.3
D	10.0	K	18.9
E	1.7	L	10.0
F	8.6	M	0.4
G	0.7	N	0.4

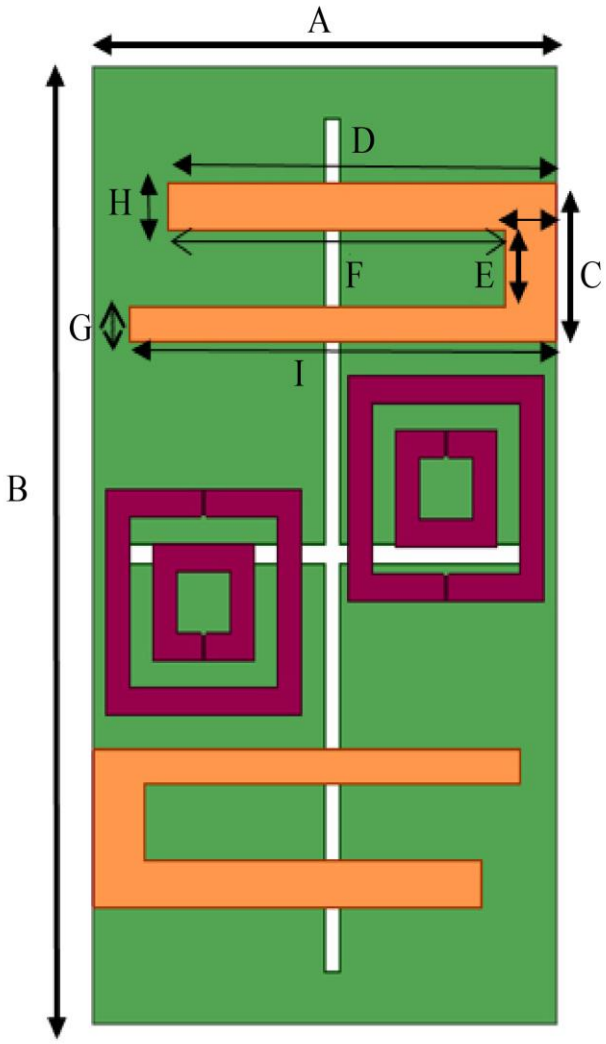

Fig. 8(d) Stage-4 of the band pass filter design

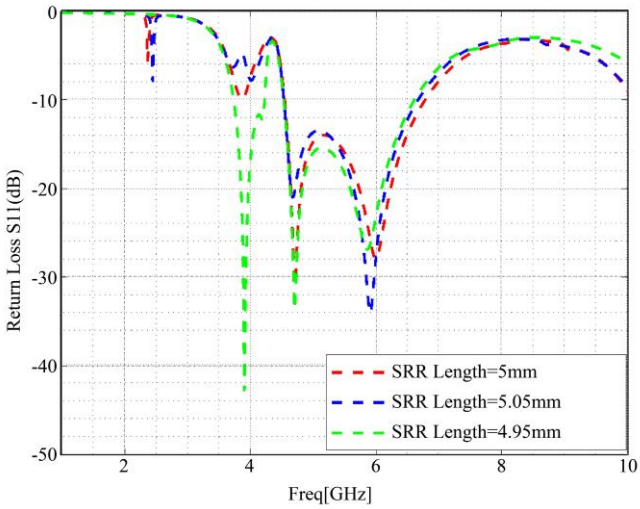

Fig. 9(a) S_{11} by varying the length of the split ring resonator used in the filter

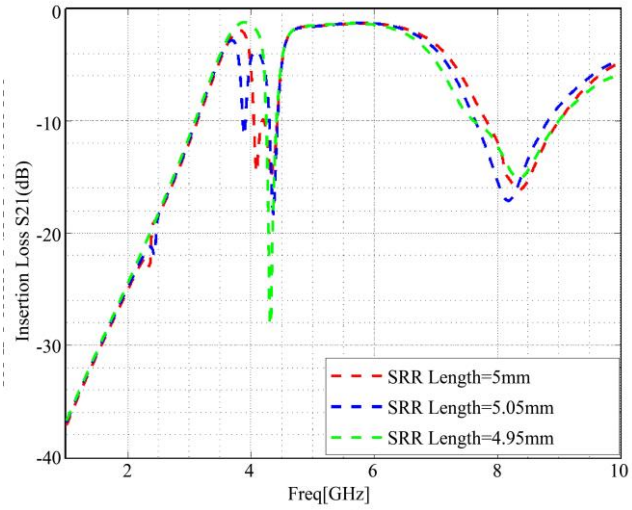

Fig. 9(b) S_{21} by varying the length of the split ring resonator used in the filter

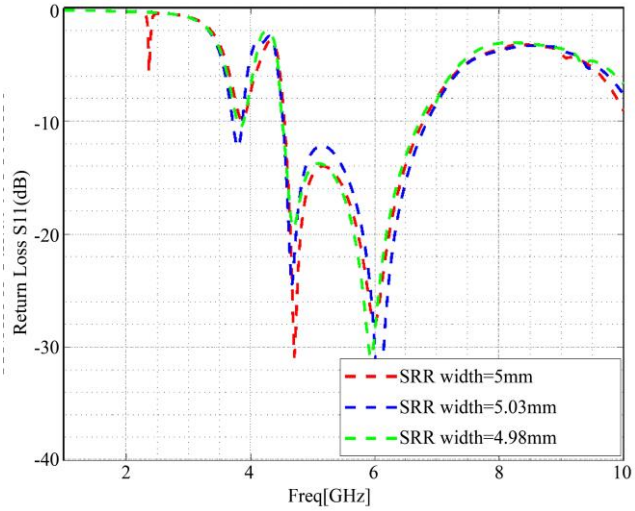

Fig. 10(a) S_{11} by varying the width of the split ring resonator used in the filter

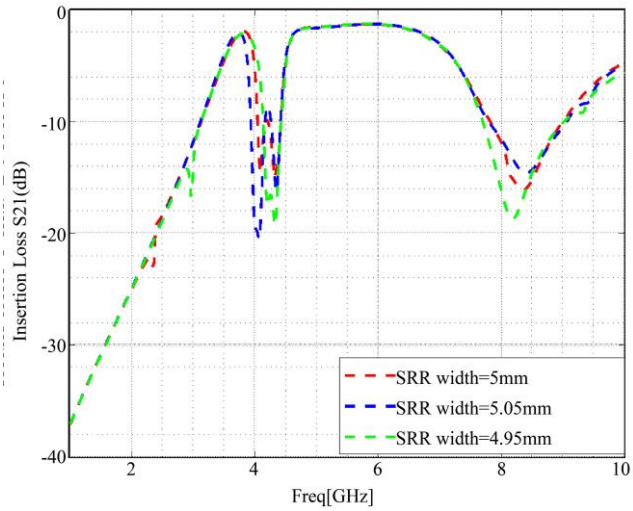

Fig. 10(b) S_{21} by varying the width of the split ring resonator used in the filter

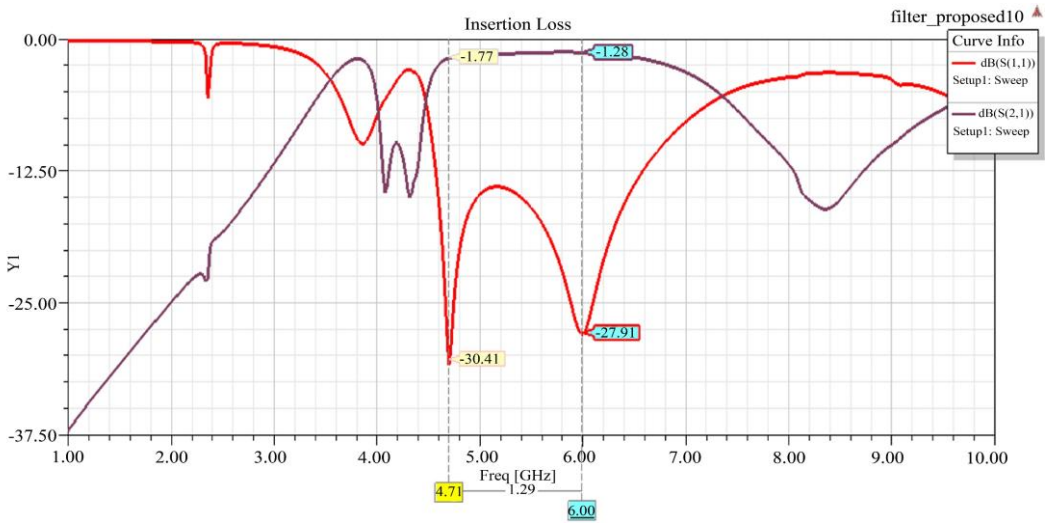

Fig. 11 Frequency response of the designed filter

5. Results

Compared to the previous work reported as indicated in Table 3, the proposed band pass filter, illustrated in Figure 8(d), having two S-DSRR, is simulated with ANSYS HFSS software and exhibits excellent pass band behaviour from 4.5 GHz to 7.5 GHz, with a bandwidth of 3 GHz and an insertion loss of 1.28dB over the pass band. The fractional bandwidth is 63%. The results indicated a sharp cut-off before and after the pass band. The results also show good return loss, implying good transmission quality across the frequency range.

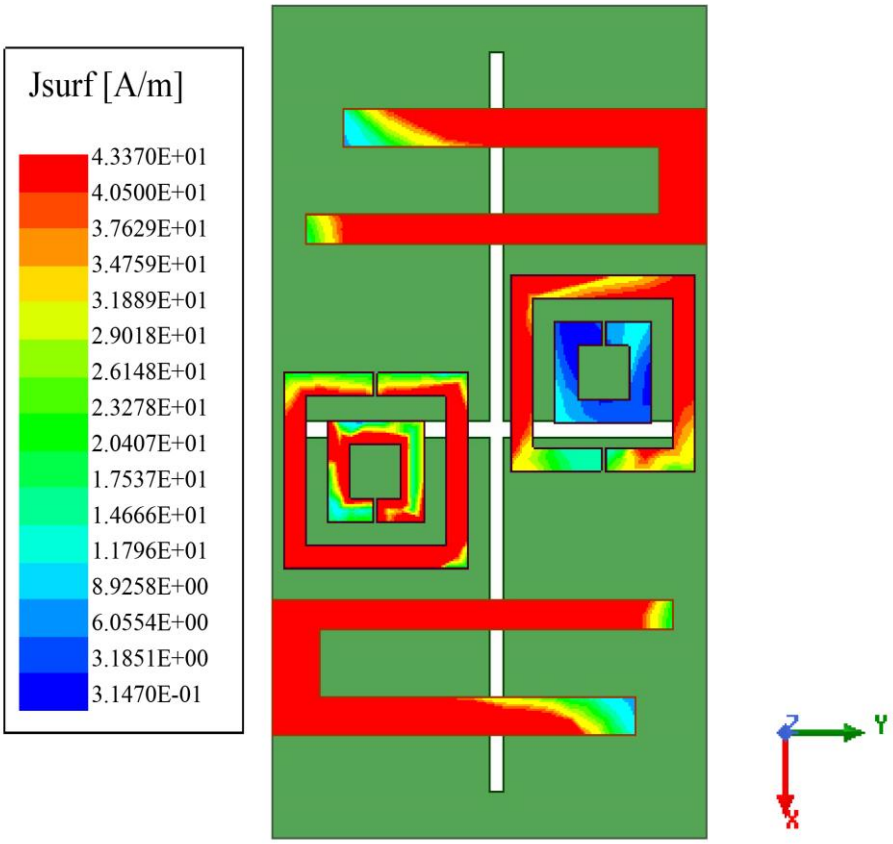

Fig. 12(a) Simulated surface current density distribution for the designed filter

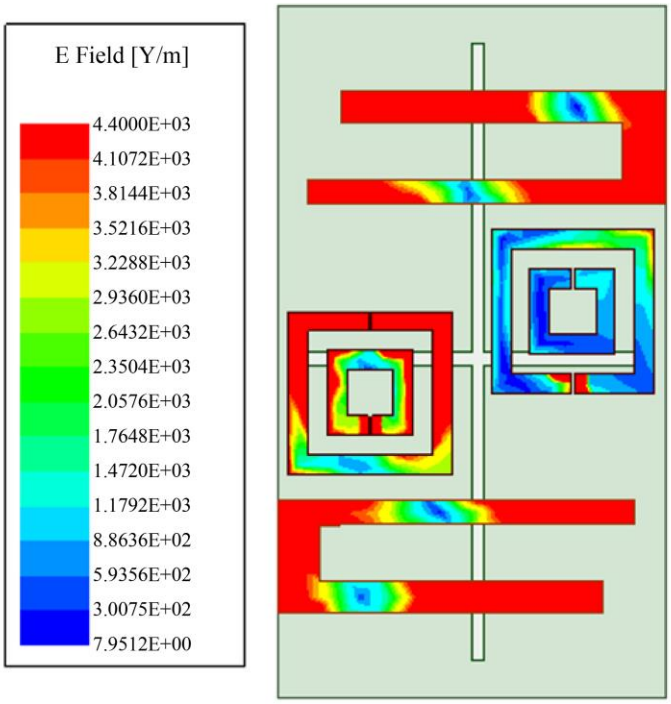

Fig. 12(b) Simulated electric field distribution for the designed filter

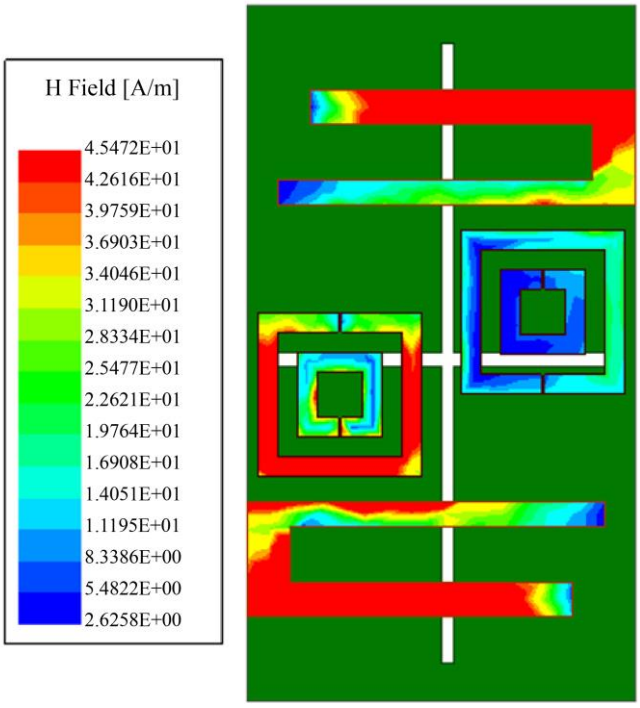

Fig. 12(c) Simulated magnetic field intensity distribution for the designed filter

The proposed band pass filter is subjected to an electromagnetic analysis using the ANSYS HFSS software. The electric field (V/m), magnetic field strength (A/m), and surface current density (A/m) are the features that are examined. Figure 12(a) displays an examination of the simulation results, indicating radio frequency power transfer from the input port to the output port by the band pass filter. The maximum surface current density is 4.3 A/m. The electric and magnetic field intensities exhibited in Figures 12(b) and 12(c) demonstrate that they are concentrated on the ring and diminish in the substrate.

Table 3. Summary of the metamaterial-based BPF design reported in previous work

Ref.	Substrate Material	Design Features	Demerits
[8]	RT/Duroid 5880 ε_r =2.2 t=0.5mm	Use of single C- SRR	• Extremely narrow BPF with FBW of 3% • Very high insertion loss of 2.8dB • Size is 25x20mm^2 • Difficult to place I/O ports due to very thin substrate
[10]	RT/Duroid 5880 ε_r =2.2 t=1.6mm	Use of tuning device of two S-DSRR	• Difficulty in tuning the varactor diode • Narrow BPF having FBW of 13% • Size is 20x15mm^2
[11]	RT/Duroid 6010 ε_r =10.2 t=1.9mm	Use of 3 S-DSRR	• Lower band coverage from 2.3-2.5GHz • Lower FBW of 8.5% • Very high insertion loss of 3.8dB • Size is 30.1x6.9mm^2
[18]	Rogers RO3010 εr =10.2 t=1.5mm	Polygon	• Complex structure to analyze • Lower band coverage from 2.2 GHz-2.5GHz • Lower FBW of 12.5% • Size is 16x8mm^2
[19]	FR4 ε_r =4.4 t=1.6mm	Use of coupled lines, stubs, S-DSRR and S-CSRR	• Lower band coverage from 0.96GHz-1.04GHz • Extremely narrow BPF with FBW of 1% • High insertion loss of 2.68dB • Size is 130x50mm^2
[20]	FR4 ε_r=4.4 t=1.6mm	Use of single S-CSRR having only negative permittivity	• Complex CSRR structure. Difficult to obtain an equivalent circuit. • Lower band coverage from 2.5-4GHz • Lower FBW of 45% • Size is 18.2x19mm^2 • Variations of physical dimensions on frequency shift, return loss, and insertion loss not discussed
[21]	FR4 ε_r =3.1 t=0.8mm	Use of two metal stubs and single C-CSRR having only negative permeability	• Complex filter structure • Bulky since the stubs are used • Lower band coverage from 4-6.5 GHz • Lower FBW of 45% • Poor BW performance using stubs • Addition of cavities to the BPF design for improving out-of-band rejection, which further makes the design more complex
[23]	FR4 ε_r =4.4 t=1.6mm	Use of single S-SRR having negative permittivity and permeability	• Complex SRR structure with 3 rings. Difficult to obtain an equivalent circuit. • Extremely narrow-band BPF having BW of 170,240 and 390 at 2.4,4.5 and 5.2GHz. • Insertion loss >2dB at 5.2GHz • Size is 40x40mm^2
[25]	FR4 ε_r =4.4 t=1.6mm	Use of single S-SRR having only negative permittivity	• Lower band coverage from 1.5-2.3GHz • Lower FBW of 40% • Size is 21x12mm^2 • Variations of physical dimensions on frequency shift, return loss, and insertion loss not discussed

6. Conclusion

The study begins by examining a split ring resonator, which belongs to the metamaterial family. An investigation is conducted on the permittivity, permeability, reflection and transmission coefficients of the metamaterial unit cell. A compact band pass filter is designed and optimized using ANSYS HFSS software, utilizing a split ring resonator. The filter design demonstrates excellent electrical performance.

The return loss at a frequency of 4.71GHz is measured to be 30.41 dB, while the insertion loss is found to be 1.77 dB. The return loss at a frequency of 6GHz is measured to be 27.91 dB, while the insertion loss is found to be 1.28 dB. The filter has a wide pass band with FBW = 63%. The electromagnetic field analysis based on the Finite Element Analysis (FEA) for the proposed band pass filter was presented, the examination of which indicated the transfer of power between the ports.

References

[1] Jeffrey G. Andrews et al., "What will 5G be?," *IEEE Journal on Selected Areas in Communications*, vol. 32, no. 6, pp. 1065-1082, 2014. [CrossRef] [Google Scholar] [Publisher Link]

[2] Xuanfeng Tong et al., "Low-Profile, Broadband, Dual-Linearly Polarized, and Wide-Angle Millimeter-Wave Antenna Arrays for Ka-Band 5G Applications," *IEEE Antennas and Wireless Propagation Letters*, vol. 20, no. 10, pp. 2038-2042, 2021. [CrossRef] [Google Scholar] [Publisher Link]

[3] Wonil Roh et al., "Millimeter-Wave Beamforming as an Enabling Technology for 5G Cellular Communications: Theoretical Feasibility and Prototype Results," *IEEE Communications Magazine*, vol. 52, no. 2, pp. 106-113, 2014. [CrossRef] [Google Scholar] [Publisher Link]

[4] Longfang Ye et al., "Substrate Integrated Plasmonic Waveguide for Microwave Bandpass Filter Applications," *IEEE Access*, vol. 7, pp. 75957-75964, 2019. [CrossRef] [Google Scholar] [Publisher Link]

[5] Yuxuan Luo et al., "A Compact Microwave Bandpass Filter Based on Spoof Surface Plasmon Polariton and Substrate Integrated Plasmonic Waveguide Structures," *Applied Physics A*, vol. 128, no. 2, pp. 1-8, 2022. [CrossRef] [Google Scholar] [Publisher Link]

[6] Gaurav Mittal, and Nagendra Prasad Pathak, "Spoof Surface Plasmon Polaritons Based Microwave Bandpass Filter," *Microwave and Optical Technology Letters*, vol. 63, no. 1, pp. 51-57, 2021. [CrossRef] [Google Scholar] [Publisher Link]

[7] Madiha Farasat et al., "A Review on 5G Sub-6 GHz Base Station Antenna Design Challenges," *Electronics*, vol. 10, no. 16, pp. 1-20, 2021. [CrossRef] [Google Scholar] [Publisher Link]

[8] Ria Lovina Defitri, and Achmad Munir, "X-Band Microstrip Narrowband BPF Composed of Split Ring Resonator," *Progress in Electromagnetics Research Symposium*, Shanghai, China, pp. 3468–3471, 2016. [CrossRef] [Google Scholar] [Publisher Link]

[9] Mohamed Hesham, and Sameh O. Abdellatif, "Compact Bandpass Filter Based on Split Ring Resonators," *International Conference on Innovative Trends in Computer Engineering*, Aswan, Egypt, pp. 301-303, 2019. [CrossRef] [Google Scholar] [Publisher Link]

[10] Ya-juan Zhao et al., "A Compact Tunable Metamaterial Filter Based on Split-Ring Resonators," *Optoelectronics Letters*, vol. 13, no. 2, pp. 120-122, 2017. [CrossRef] [Google Scholar] [Publisher Link]

[11] Mohamad Syahral, and Achmad Munir, "Development of Multiple Elements of SRR-Based Bandpass Filter," *Proceeding of 2016 10th International Conference on Telecommunication Systems Services and Applications*, Denpasar, Indonesia, pp. 1-4, 2016. [CrossRef] [Google Scholar] [Publisher Link]

[12] Zenal Aripin et al., "Compact SRR-Based Microstrip BPF for Wireless Communication," *2nd International Conference on Information Technology, Computer, and Electrical Engineering*, Semarang, Indonesia, pp. 474-477, 2015. [CrossRef] [Google Scholar] [Publisher Link]

[13] Nor Hidayah Daud et al., "Integration of Split Ring Resonators (SRRs) to UHF RFID Tag Antenna for Size Reduction," *2014 4th International Conference on Engineering Technology and Technopreneuship*, Kuala Lumpur, Malaysia, pp. 204-208, 2014. [CrossRef] [Google Scholar] [Publisher Link]

[14] Jonathan Carver, Vianney Reignault, and Frédérique Gadot, "Engineering of the Metamaterial-Based Cut-Band Filter," *Applied Physics A*, vol. 117, no. 2, pp. 513-516, 2014. [CrossRef] [Google Scholar] [Publisher Link]

[15] Philippe Gay-Balmaz, and Olivier J.F. Martin, "Electromagnetic Resonances in Individual and Coupled Split-Ring Resonators," *Journal of Applied Physics*, vol. 92, no. 5, pp. 2929-2936, 2002. [CrossRef] [Google Scholar] [Publisher Link]

[16] A.M. Nicolson, and G.F. Ross "Measurement of the Intrinsic Properties of Materials by Time-Domain Techniques," *IEEE Transactions on Instrumentation and Measurement*, vol. 19, no. 4, pp. 377-382, 1970. [CrossRef] [Google Scholar] [Publisher Link]

[17] Dubey Suhmita Umeshkumar, and Manish Kumar, "Design of an Ultra-Wideband Bandpass Filter for Millimeter Wave Applications," *Journal of Telecommunication, Electronic and Computer Engineering*, vol. 10, no. 3, pp. 57-60, 2018. [Google Scholar] [Publisher Link]

[18] A.J. Salim et al., "A Polygonal Open-Loop Resonator Compact Bandpass Filter for Bluetooth and WLAN Applications," *IOP Conference Series: Materials Science and Engineering*, vol. 433, no. 1, pp. 1-9, 2018. [CrossRef] [Google Scholar] [Publisher Link]

[19] Zaid A. Abdul Hassain, Amer Abbood AL-Behadili, and Adham R. Azeez, "First Order Parallel Coupled BPF with Wideband Rejection Based on SRR and CSRR," *Telkomnika (Telecommunication Computing Electronics and Control)*, vol. 17, no. 6, pp. 2704-2712, 2019. [CrossRef] [Google Scholar] [Publisher Link]

[20] Badr Nasiri et al., "Band-Pass Filter Based on Complementary Split Ring Resonator," *Telkomnika (Telecommunication Computing Electronics and Control)*, vol. 18, no. 3, pp. 1145-1149, 2020. [CrossRef] [Google Scholar] [Publisher Link]

[21] Kada Becharef et al., "Design and Simulation of a Broadband Bandpass Filter Based on Complementary Split Ring Resonator Circular "CSRRs"," *Wireless Personal Communications*, vol. 111, no. 3, pp. 1341-1354, 2020. [CrossRef] [Google Scholar] [Publisher Link]

[22] Ismail Topaloglu, "3D Electromagnetic Analysis and Optimization of Metamaterial Constructed by SRR Using the MOGA Algorithm for Performance Improvement," *Duzce University Journal of Science and Technology*, vol. 9, no. 3, pp. 34-47, 2021. [CrossRef] [Google Scholar] [Publisher Link]

[23] K.V. Vineetha, M. Siva Kumar, and B.T.P. Madhav, "Analysis of Triple Band Split Ring Resonator Based Microstrip Bandpass Filter," *Journal of Physics: Conference Series*, vol. 1804, no. 1, pp. 1-6, 2021. [CrossRef] [Google Scholar] [Publisher Link]

[24] K. Sagadevan, D.S. Kumar, and S. Rajagopalan, "The Design of Split Ring Resonator (SRR) Based Terahertz Bandpass Filter and Comparison of Various Types of Filters," *Journal of Physics: Conference Series*, vol. 1717, no. 1, pp. 1-7, 2021. [CrossRef] [Google Scholar] [Publisher Link]

[25] Badr Nasiri, Ahmed Errkik, and Jamal Zbitou, "Microstrip Band-Stop Filter Based on Double Negative Metamaterial," *International Journal of Electrical and Computer Engineering*, vol. 12, no. 2, pp. 1579-1584, 2022. [CrossRef] [Google Scholar] [Publisher Link]

[26] Viktor G. Veselago, "The Electrodynamics of Substances with Simultaneously Negative Values of ε and μ," *Soviet Physics Uspekhi*, vol. 10, no. 4, pp. 509-514, 1968. [CrossRef] [Google Scholar] [Publisher Link]

[27] J.B. Pendry et al., "Magnetism from Conductors and Enhanced Nonlinear Phenomena," *IEEE Transactions on Microwave Theory and Techniques*, vol. 47, no. 11, pp. 2075-2084, 1999. [CrossRef] [Google Scholar] [Publisher Link]

[28] D.R. Smith et al., "Electromagnetic Parameter Retrieval from Inhomogeneous Metamaterials," *Physical Review E Covering Statistical, Nonlinear, Biological, and Soft Matter Physic*, vol. 71, no. 3, pp. 1-11, 2005. [CrossRef] [Google Scholar] [Publisher Link]

[29] D.R. Smith et al., "Composite Medium with Simultaneously Negative Permeability and Permittivity," *Physical Review Letters*, vol. 84, no. 18, pp. 4184-4187, 2000. [CrossRef] [Google Scholar] [Publisher Link]

[30] Seif Naoui, Lassaad Latrach, and Ali Gharsallah, "Equivalent Circuit Model of Double Split Ring Resonators," *International Journal of Microwave and Optical Technology*, vol. 11, no. 1, pp. 1-6, 2016. [Google Scholar] [Publisher Link]

[31] Mukesh Kumar Khandelwal, Binod Kumar Kanaujia, and Sachin Kumar, "Defected Ground Structure: Fundamentals, Analysis, and Applications in Modern Wireless Trends," *International Journal of Antennas and Propagation*, vol. 2017, no. 1, pp. 1-22, 2017. [CrossRef] [Google Scholar] [Publisher Link]